

Biophysical and molecular comparison of sodium current in cells isolated from canine atria and pulmonary vein

Hector Barajas-Martinez¹ · Robert J. Goodrow¹ · Dan Hu¹ · Payal Patel¹ · Mayurika Desai¹ · Brian K. Panama¹ · Jacqueline A. Treat¹ · Gary L. Aistrup¹ · Jonathan M. Cordeiro¹

Received: 26 July 2016 / Revised: 8 February 2017 / Accepted: 10 February 2017 / Published online: 27 February 2017
© Springer-Verlag Berlin Heidelberg 2017

Abstract The collar of the pulmonary vein (PV) is the focal point for the initiation of atrial arrhythmias, but the mechanisms underlying how PV cells differ from neighboring left atrial tissue are unclear. We examined the biophysical and molecular properties of I_{Na} in cells isolated from the canine pulmonary sleeve and compared the properties to left atrial tissue. PV and left atrial myocytes were isolated and patch clamp techniques were used to record I_{Na} . Action potential recordings from either tissue type were made using high-resistance electrodes. mRNA was determined using quantitative RT-PCR and proteins were determined by Western blot. Analysis of the action potential characteristics showed that PV tissue had a lower V_{max} compared with left atrial tissue. Fast I_{Na} showed that current density was slightly lower in PV cells compared with LA cells (-96 ± 18.7 pA/pF vs. -120 ± 6.7 pA/pF, respectively, $p < 0.05$). The recovery from inactivation of I_{Na} in PV cells was slightly slower but no marked difference in steady-state inactivation was noted. Analysis of late I_{Na} during a 225-ms pulse showed that late I_{Na} was significantly smaller in PV cells compared to LA cells at all measured time points into the pulse. These results suggest PV cells have lower density of both peak and late I_{Na} . Molecular analysis of Nav1.5 and the four beta subunits showed lower levels of Nav1.5 as well as Nav β 1 subunits, confirming the biophysical findings. These data show that a lower density of I_{Na} may lead to depression of excitability and predispose the PV collar to re-entrant circuits under pathophysiological conditions.

Keywords Sodium current · Atria · Pulmonary vein · Patch clamp · Action potentials

Introduction

Atrial fibrillation (AF) is the most common arrhythmia in the clinical setting, affecting about 2.5 million people in the USA. There are several treatment options for the effective treatment and management of AF, one being antiarrhythmic drug therapy. Among the current strategies is the use of antiarrhythmic agents that preferentially affect atrial tissue rather than ventricular electrophysiology. These treatment strategies include inhibition of the ultrarapid delayed rectified potassium current (I_{Kur}) which is thought to be present in atria but not ventricles [15, 16]. More recent treatment involves the use of atrial selective sodium channel blockers to suppress AF [5, 36].

Previous studies from our labs have shown there are tissue-specific differences of I_{Na} in the canine heart. In ventricles for example, epicardial I_{Na} has a significantly more negative steady-state mid-inactivation potential compared with endocardial [11]. In addition and in agreement with other studies [5, 27], we found that atrial I_{Na} has a higher current density and a more negative steady-state mid-inactivation potential compared to ventricular I_{Na} [7]. The negative steady-state mid-inactivation potential will tend to leave a larger fraction of atrial I_{Na} channels in an inactivated state resulting in a larger pool of inactivated channels. Pathological conditions such as ischemia or acidosis may further reduce I_{Na} and cardiac conduction [19, 31].

Abnormal electrical activity localized in the collar of the pulmonary vein (PV) has been shown to initiate many of the AF episodes in humans. The discovery that the PV area initiates many AF episodes has led to the novel work of Haissaguerre et al. who successfully isolated and ablated the

✉ Jonathan M. Cordeiro
jcordeiro@mmrl.edu

¹ Department of Experimental Cardiology, Masonic Medical Research Laboratory, 2150 Bleecker Street, Utica, NY 13501, USA

PV area resulting in a marked suppression and termination of AF episodes in patients [20, 25]. However, the mechanism by which PV tissue is the focal point of AF is not completely understood. Previous studies have looked at some of the electrophysiological characteristics in the two cell types, but with differing results [12, 14].

In this study, we isolated myocytes from the LA and PV region and examined the molecular and biophysical differences of peak and persistent (or late) Na^+ current. Results of our study showed that PV cells exhibited a lower peak Na^+ current compared to left atrial cells; no effect on steady-state activation but a small shift in inactivation was observed. Recovery from inactivation in PV cells was slightly slowed. The density of persistent or late I_{Na} was also slightly lower in PV vs. atrial cells. Molecular analysis revealed PV cells had a lower expression of Nav1.5 consistent with the lower I_{Na} density. In addition, differences in the ratios of beta subunits between the two cell types were noted. Our observations suggest that Na^+ current is smaller in PV cells compared to LA. These observations suggest that certain pathophysiological conditions would further reduce Na^+ current in PV cells, resulting in conditions favorable for reentry to develop around the PV collar.

Methods

Adult mongrel dogs of either sex (age 1–4 years) were used for all experiments, and this investigation conforms to the Guide for Care and Use of Laboratory Animals published by the National Institutes of Health (The Eighth Edition of the *Guide for the Care and Use of Laboratory Animals* (NRC 2011)). All protocols were approved by the Institutional Animal Care and Use Committee. Dogs were anticoagulated with heparin and anesthetized with pentobarbital (30–35 mg/kg, i.v.). The chest was open via a left thoracotomy, the heart excised, and placed in cold cardioplegic solution of the following composition (in mM): NaCl 129, KCl 12, NaH_2PO_4 0.9, NaHCO_3 20, CaCl_2 1.8, MgSO_4 0.5, and glucose 5.5.

Isolated tissue action potential recordings

Atrial or pulmonary vein tissue was isolated and superfused with oxygenated (95% O_2 /5% CO_2) Tyrode's solution of the following composition (in mM): NaCl 129, KCl 4, NaH_2PO_4 0.9, NaHCO_3 20, CaCl_2 1.8, MgSO_4 0.5, and glucose 5.5, pH = 7.4. All preparations were allowed to equilibrate until the action potentials reached steady state. Tissues were stimulated at basic cycle lengths (BCL) of 500–2000 ms (2–5 ms duration) delivered through silver bipolar electrodes. Transmembrane action potentials were recorded from tissue using glass microelectrodes filled with 2.7 M KCl (10–

30 M Ω) connected to a high input-impedance amplification system (Electro 705 Electrometer, World Precision Instruments). The signals were digitized at 20 kHz (model 1401 AD/DA system, Cambridge Electronic Designs (C.E.D.)) and analyzed using the Spike 2 acquisition software (C.E.D.).

Isolated atrial myocyte preparation

Atrial myocytes were prepared from canine hearts using techniques described previously [6, 7]. Briefly, the left atria were dissected and perfused through the ostium of the coronary artery. During the cannulation procedure, the preparations were perfused with cardioplegic solution before switching to a nominally Ca^{2+} -free solution (mM): NaCl 129, KCl 5.4, MgSO_4 2.0, NaH_2PO_4 0.9, glucose 5.5, and NaHCO_3 20, bubbled with 95% O_2 /5% CO_2 containing 0.1% BSA for a period of about 5 min. The preparation was then subjected to enzyme digestion with the nominally Ca^{2+} -free solution supplemented with 0.5 mg/ml collagenase (type II, Worthington), 0.1 mg/ml protease (type XIV, Sigma), and 1 mg/ml BSA for 8–12 min. The pectinate muscle was then isolated and placed in a separate beaker. Tissue was minced and incubated in fresh buffer containing 0.5 mg/ml collagenase, 1 mg/ml BSA and agitated. The supernatant was filtered, centrifuged at 200 rpm for 2 min, and the myocyte-containing pellet was stored in 0.5 mM Ca^{2+} HEPES buffer at room temperature.

Isolation of pulmonary vein cells

Pulmonary vein (PV) cells were prepared by the chunk method [6, 13]. Briefly, the collar of the pulmonary vein was dissected out, placed in a small dish, and minced. Tissue was then subjected to enzyme digestion with nominally Ca^{2+} -free solution supplemented with 1.0 mg/ml collagenase (type II, Worthington) and 30 mM 2,3-butanedione monoxime (BDM) at 36 °C. Dissociation of cells from the tissue was aided by agitation of the enzyme solution with a small stir bar. Periodically, the enzyme solution containing PV cells in suspension was removed and added to a modified storage solution (described above). Fresh enzyme solution was added to the undigested PV tissue to maintain a volume of 2 ml. Digestion of the PV tissue into individual myocytes typically required 15–45 min. Cells were kept in low- Ca^{2+} storage solution at room temperature until use.

Voltage clamp recordings of peak I_{Na}

Early sodium current, I_{Na} , was measured as previously described with minor modifications [3, 7, 11]. Experiments were performed using a MultiClamp 700A (Molecular Devices, Foster City, CA). Command voltages were delivered and data acquired via a DigiData 1322 computer interface using

pClamp 9 (Molecular Devices) with data stored on a computer hard disk. Patch pipettes were pulled from borosilicate glass (1.5 mm o.d. and 1.1 mm i.d.) on a Model PP-830 vertical puller (Narashige Instruments, Japan). The electrode resistance was 0.9–2.0 M Ω when filled with the internal solution (see below). The membrane was ruptured by applying negative pressure and series resistance compensated by 75 to 80%. Whole cell current data was acquired at 20–50 kHz and filtered at 5 kHz. The capacitance of the cell was measured by integrating the transient charge following application of a –5-mV voltage clamp step. Currents were normalized to cell capacitance and expressed as density (pA/pF).

External solution contained the following (in mM): choline Cl 120, NaCl 10, Na⁺ acetate 2.8, CaCl₂ 0.5, KCl 4, MgCl₂ 1.5, CoCl₂ 1, glucose 10, HEPES 10, NaOH 5, and BaCl₂ 0.1, pH adjusted to 7.4 with NaOH/HCl. The pipette solution contained the following (mM): NaCl 15, CsF 120, MgCl₂ 1, KCl 5, HEPES 10, Na₂ATP 4, and EGTA 10, pH adjusted to 7.2 with CsOH. Peak sodium current was dramatically reduced in the low extracellular sodium to ensure adequate voltage control, as gauged by the slope of a Boltzmann fit to the steady-state activation curve [26]. When measuring sodium channel kinetics and density, the holding potential was –120 mV to recruit all available sodium channels. In addition, recordings of I_{Na} were made at least 5 min after rupture to minimize the effects of time-dependent negative shift of steady-state inactivation that occurs in conventional voltage clamp experiments. Whole cell currents were analyzed using the *Clampfit* analysis program from pClamp 9 (Molecular Devices).

Voltage clamp recordings of late I_{Na}

Late I_{Na} density was measured in full external Na⁺ [31, 35] with minor modifications [4]. The external solution contained the following (in mM): 125 NaCl, 2.8 Na-Acetate, 4 KCl, 0.5 CaCl₂, 1.5 MgCl₂, 10 glucose, 5 TEA-Cl, 2 4-aminopyridine, 0.5 BaCl₂, 1 CoCl₂, and 10 HEPES (pH = 7.4 with NaOH). Pipette solution contained the following (mM): NaCl 15, CsF 120, MgCl₂ 1, KCl 5, HEPES 10, Na₂ATP 4, and EGTA 10, pH adjusted to 7.2 with CsOH.

Late I_{Na} density was recorded in cells that were held at –80 mV. To remove steady-state inactivation and recruit all Na⁺ channels, a pulse to –120 mV was applied before a 225-ms pulse to –30 mV. The protocol was performed under control followed by rapid application of 10 μ M TTX. Late I_{Na}, characterized as the TTX-sensitive difference current, was measured at various time intervals throughout the 225-ms step.

Quantitative real-time PCR

qPCR analysis was performed with the QuantStudio 6 Flex Real-Time PCR System (Applied Biosystems, CA, USA).

Total RNA was extracted with RNAeasy Micro (cells) and Mini or Trizol (tissues) Kits (Qiagen, CA, USA). One hundred nanograms total RNA from each of the pooled PVC cells/tissues or atrial tissue samples were reverse transcribed with SuperScript™ First Strand Synthesis System for RT-PCR (Invitrogen, CA, USA). Real-time PCR was performed in triplicates for every sample using primers listed in Table 1. Using SYBR Green/ROX probe (Thermo Fisher, MA, USA), averaged Ct values of each qPCR reaction from the target gene were normalized with the average Ct values of the housekeeping gene 18S, which ran in the same reaction plate to obtain the Δ Ct value. Expression was normalized from Δ Ct values for each gene against the reference housekeeping gene 18S, using the formula $2^{-\Delta\Delta Ct} (1 \times 10^6)$ [28]:

Western blotting

Protein analysis was performed as previously described with minor modifications [3, 8, 21]. Atrial and PV tissue from 3 dogs was snap-frozen in liquid nitrogen and stored in –80 °C prior to protein isolation. Membrane proteins were isolated using the Proteo Extract Native Membrane Kit (Calbiochem) according to the manufacturer's protocol. Protein concentration was determined by BCA assay (Pierce BCA Protein Assay). Samples were denatured 10 min at 65 °C with 355 mM β -mercaptoethanol, separated on precast polyacrylamide 4–15% Tris-HCl gels (Bio-Rad) and transferred to polyvinylidene fluoride (PVDF) membranes. The PVDF membranes were incubated overnight at 4 °C with the following primary antibodies: rabbit polyclonal anti-Nav1.5 (1:3000 dilution, Sigma-Aldrich), rabbit polyclonal anti-Nav β 1 (1:3000 dilution, Alomone Labs), and mouse monoclonal anti-pan cadherin (1:3000, Abcam) was used as a loading control. Secondary antibodies were HRP-conjugated goat anti-rabbit IgG (1:10,000, Bio-Rad) and goat anti-mouse IgG (1:10,000, Bio-Rad). The proteins were visualized using the Bio-Rad ChemiDoc Imaging System.

Statistics

Results from pooled data are presented as mean \pm SEM. Statistical analysis was performed using an ANOVA test followed by a Student-Newman-Keuls test or a Student's *t* test, as appropriate, using the SigmaStat software. A *p* < 0.05 was considered statistically significant.

Results

As an initial basis of comparison, APs and V_{max} were simultaneously recorded in either left atrial or PV tissues. Figure 1 shows AP recordings (top traces) from either a pulmonary vein (panel a) or left atrial (panel b) preparation paced at

Table 1 Oligonucleotide sequences of the primers used for RT-PCR

Gene name	Forward primer	Reverse primer
SCN5A	CACCATGTGCATCGTCCTTAAC	CCATGAGGCTCAGGATGACAAT
SCN1B	TCTTCTTCGAGAACTACGAG	CATACATCATGATCTCCGAC
SCN2B	TACACAGTGAACCACAAAC	CAGGTTAATGATCTTCATGC
SCN3B	ATATTGCTACAGGAAGGTCTC	GCTCTCTTTGTTCTCTGA
SCN4B	AAATTCAGCTCATAGACGG	CTTCTTTAGTGGAACCCCTC
18S	CGCCGCTAGAGGTTGAAATTC	TCCGACTTTCGTTCTTGATTAATG

various cycle lengths. Analysis of the AP characteristics showed that the average resting membrane potential was -81.7 ± 2.35 mV ($n = 10$) for PV preparations and -82.9 ± 1.5 mV for LA tissue ($n = 5$). Also, a statistically significant prolongation of APD₈₅ in atrial compared to PV tissue was noted at all three pacing cycle lengths (Fig. 1c). In addition, APD was longer in atrial tissue at several other cycle

lengths. The upstroke velocity (an index of I_{Na}) showed that LA and PV sleeves had a similar V_{max} (202.8 ± 49.4 V/s vs. 189.5 ± 40.7 V/s, respectively).

The small differences in upstroke velocity as well as the greater APD observed in atrial tissue compared to PV sleeves may suggest that both peak and later Na^+ current in atrial tissue may be larger. To test this hypothesis, we measured both

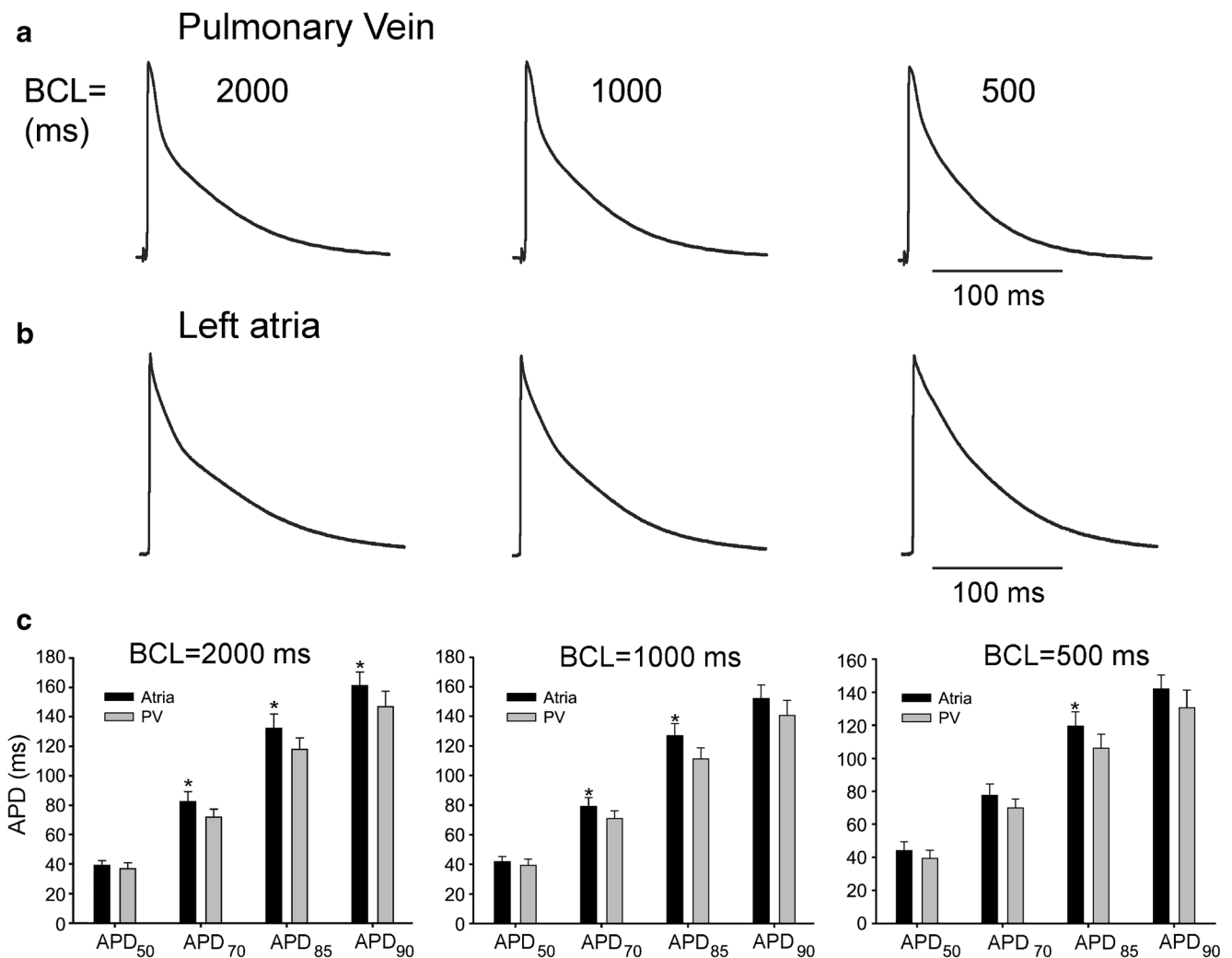


Fig. 1 Representative action potentials recorded from pulmonary vein (a) or left atrial tissue (b) at three stimulation rates. Mean data summarizing APD at different repolarization time points in atria and PV tissue (c)

peak and late I_{Na} in the two cell types. Peak I_{Na} was measured in low extracellular sodium buffer to ensure adequate voltage control. Representative I_{Na} traces recorded from an atrial and PV cell are shown (Fig. 2a, b). Analysis of the I-V relation (Fig. 2c) showed that peak I_{Na} density was larger in atrial cells compared to PV cells (-120 ± 6.7 pA/pF vs. -96 ± 18.7 pA/pF, respectively, $p < 0.05$) but no shift in the activation threshold was noted. We also measured steady-state activation from the I-V curves. Chord conductance was determined using the ratio of current to the electromotive potential for the cells shown in panel c and a Boltzmann curve was fit to the data. Analysis of steady-state activation showed mid-activation voltages ($V_{1/2}$) of -45.2 ± 0.42 mV, $k = 5.2 \pm 0.36$ for atria and -43.7 ± 0.41 mV, 5.91 ± 0.37 for PV cells (Fig. 2d).

We next evaluated steady-state inactivation in atrial and PV cells. Peak current following a 500 ms prepulse was normalized to the maximum current and plotted as a function of the prepulse voltage. A Boltzmann function was then fit to the data. Representative traces recorded from atrial (Fig. 3a) and PV

cells (Fig. 3b) are shown. Figure 3c shows there was a small but significant difference in the mid-inactivation potential between the two cell types ($V_{1/2} = -80.1 \pm 0.07$ mV, $k = 4.91 \pm 0.06$ for atrial vs. $V_{1/2} = -82.0 \pm 0.21$ mV, $k = 5.05 \pm 0.18$ for PV, $p < 0.05$). These results show that PV cells exhibit a decrease density in peak I_{Na} and a small negative shift in steady-state inactivation.

In the next series of experiments, we determined if recovery from inactivation of I_{Na} was dramatically different in atrial and PV cells. Recovery was determined using a standard double pulse protocol separated by various time intervals (voltage clamp protocol shown at the top of the figure). Representative traces recorded from a PV and atrial cell showing I_{Na} recovery at $h_p = -100$ mV (Fig. 4a–b). Recovery of I_{Na} was slightly slower in PV cells compared to atria at all three holding potentials examined. In atria, reactivation of I_{Na} at $h_p = -100$ mV had a fast and slow phase of recovery as follows: (i) $\tau_1 = 7.86 \pm 0.47$ ms and $\tau_2 = 37.0 \pm 2.02$ ms. In contrast, PV cells exhibited a slower recovery from inactivation as

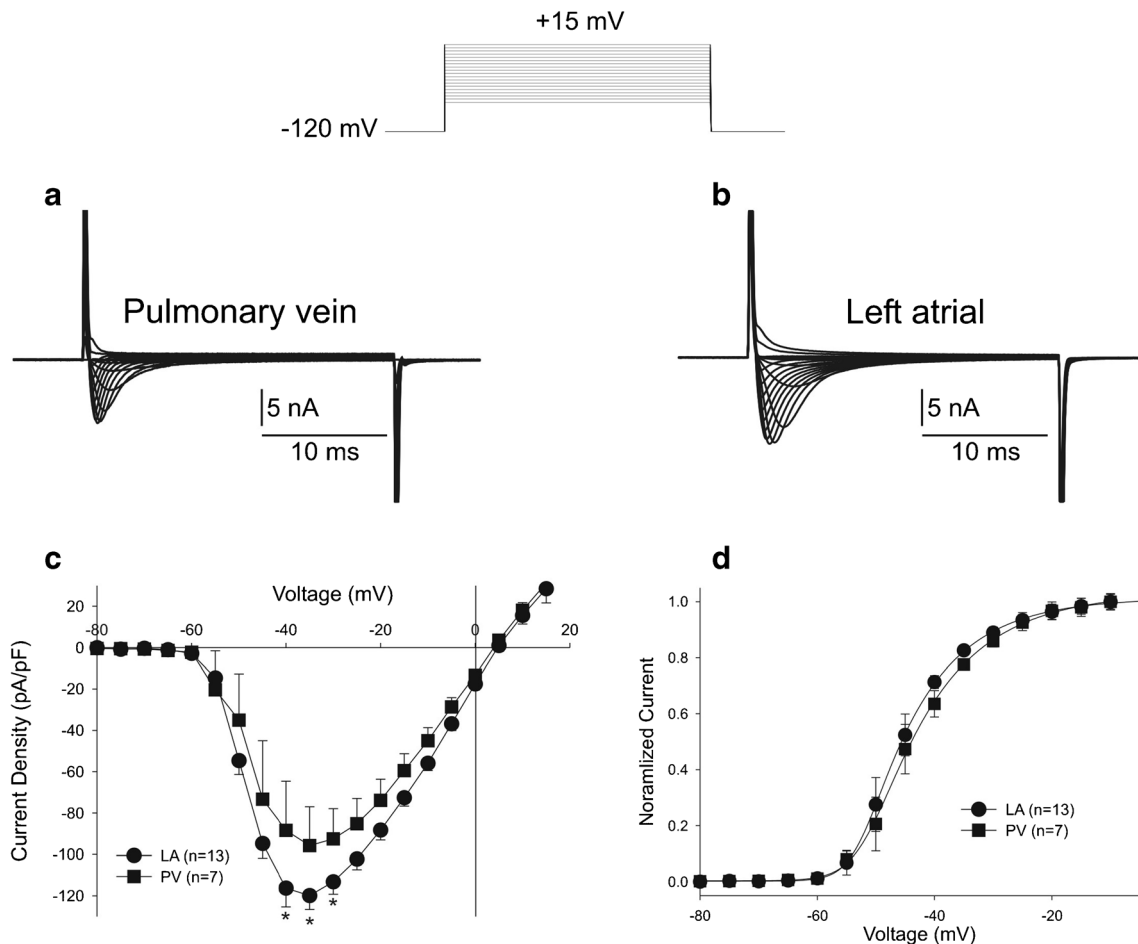
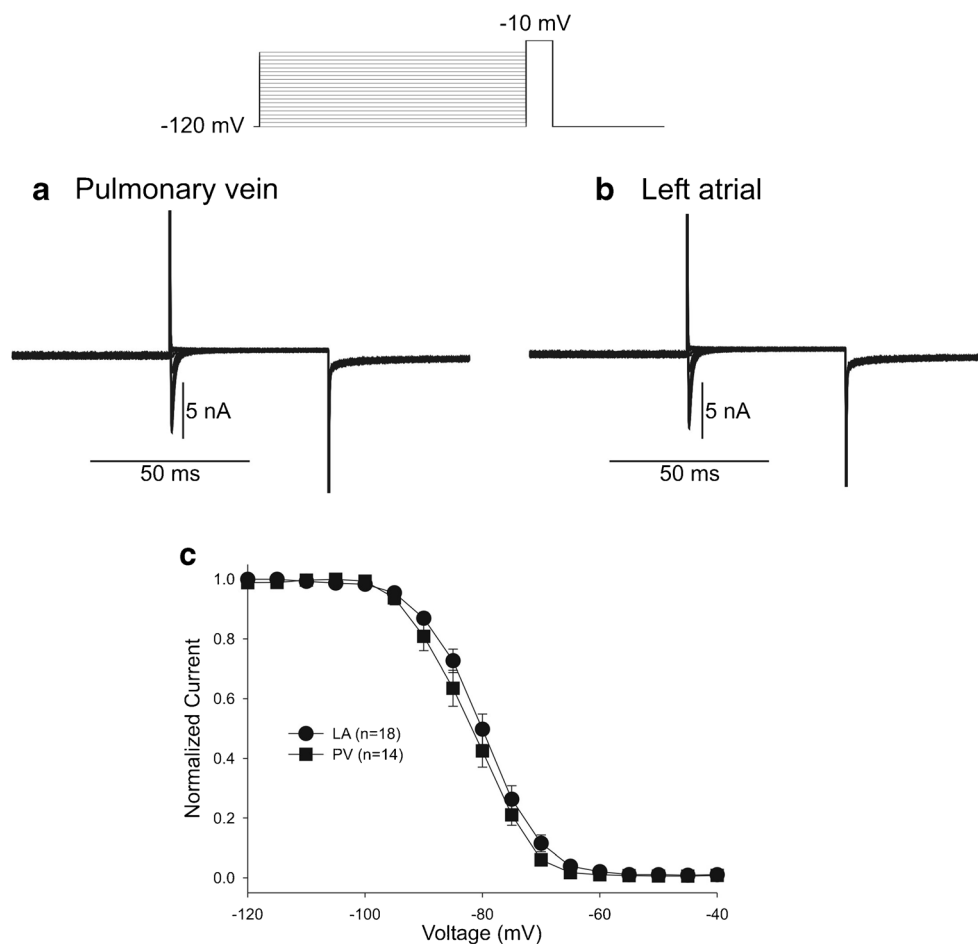


Fig. 2 Representative I_{Na} recordings from a PV (a) and left atrial myocyte (b). Current recordings were obtained at test potentials between -80 and 15 mV in 5 -mV increments. The holding potential was -120 mV. c I-V relation for PV ($n = 7$) and left atrial myocyte ($n = 13$) showing a small but significant reduction in I_{Na} magnitude in

PV cells. d Steady-state activation relation for PV and atrial cells. Chord conductance was determined using the ratio of current to the electromotive potential for the cells shown in a and b. Data were normalized and plotted against their test potential

Fig. 3 Representative steady-state inactivation recordings from a PV (**a**) and left atrial cell (**b**). At the top of the figure is the voltage clamp protocol. Peak current was normalized to their respective maximum values and plotted against the conditioning potential. The mean data for the steady-state inactivation relation is shown (**c**)



follows: (i) $\tau_1 = 8.15 \pm 1.43$ ms and $\tau_2 = 41.43 \pm 2.65$ ms ($p = \text{NS}$ for fast phase; $p < 0.05$ for slow phase)

The results thus far show that peak I_{Na} density was smaller in atrial cells vs. PV cells. Since peak I_{Na} was smaller, we surmised that persistent (or late) I_{Na} was also reduced. We next measure late I_{Na} during a 225-ms test pulse in full external Na^+ at 37 °C. Currents measured from a control PV myocyte measured at -30 mV are shown in the absence of drug and after application of 10 μM TTX (Fig. 5a). Subtraction of the TTX trace from the drug-free trace results in the TTX-sensitive difference current shown in Fig. 5b. Similar subtractions were performed in atrial and PV cells and the mean TTX-sensitive current are summarized (Fig. 5b–c). Analysis of late I_{Na} during a 225-ms pulse showed the atrial cells had a significantly larger late I_{Na} compared to PV cells at all measured time points (Fig. 5c).

Our biophysical results show a lower density of I_{Na} in PV cells as well as differences in the biophysical properties between the two cell types. We next examined mRNA gene expression levels of *SCN5A* (encoding $\text{Na}_v1.5$) and *SCN1B-4B* (encoding $\beta 1-4$ subunit isoforms) in atrial and PV cardiomyocytes. The expression for each Na^+ channel subunit was compared to the housekeeping gene (18S) using

quantitative RT-PCR analysis (Fig. 6). We found that the alpha subunit, *SCN5A*, was the highest gene expressed compared with the beta subunits in the canine heart. These results show a significant higher expression of *SCN5A* and *SCN1B* fold in the atria compared to the PVC. However, PV tissue showed higher levels of *SCN2B* and *SCN4B* compared to atria.

To determine if differences in transcript was paralleled at the protein level, we assessed Nav1.5 and Nav $\beta 1$ by Western blot analysis (Fig. 7). Representative Western blot gels are shown in Fig. 7a. A diffuse doublet band (denser high band) was discernible in the anti-Nav1.5 blot, and 3–5 bands were discernible in the anti-Nav $\beta 1$ blot, consistent with previous reports indicating differential glycosylation states [34]. The anti-Nav1.5 blot tended to indicate more Nav1.5 in the PV than in LA, and the anti-Nav $\beta 1$ blot tended to indicate less Nav $\beta 1$ in the PV than in the LA. However, densitometry analysis indicated that neither was statistically significant (Fig. 7b).

Discussion

The results of our study demonstrated important functional differences in both peak and late I_{Na} in PV tissue vs. atria.

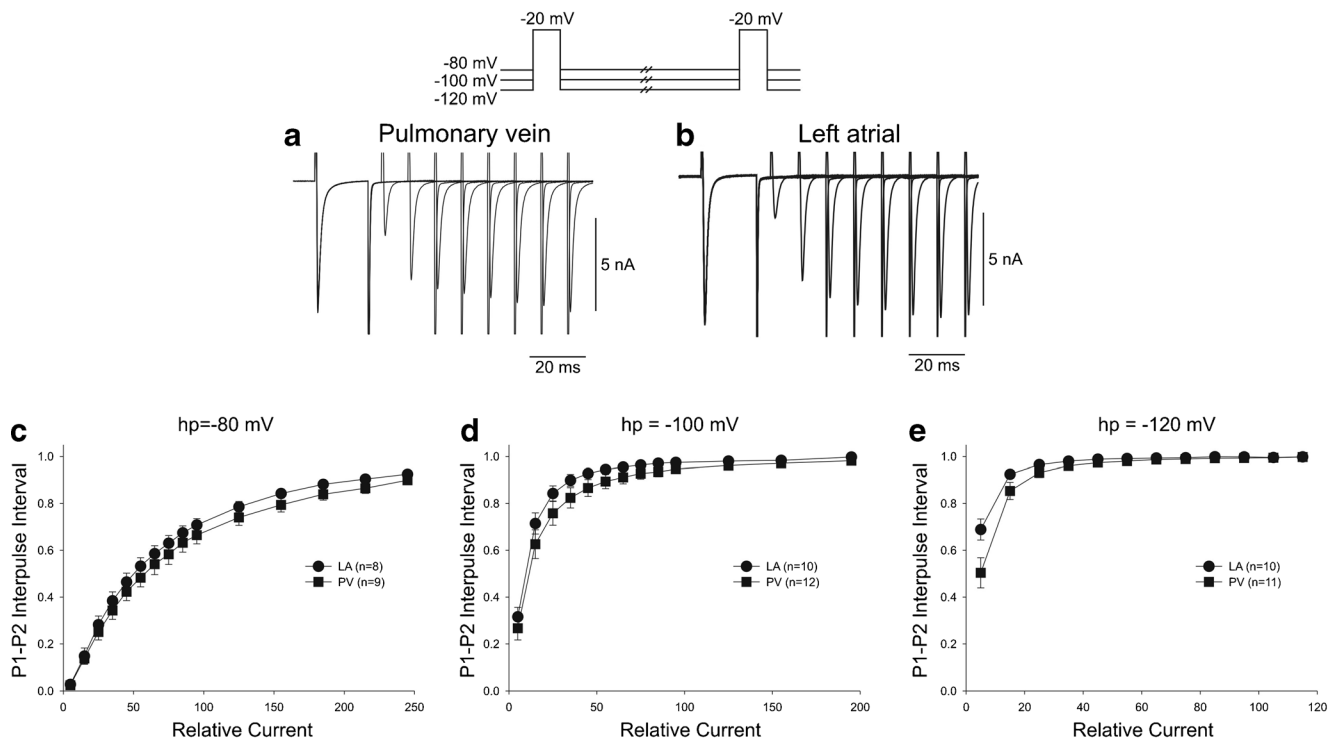


Fig. 4 Representative traces recorded from a PV (**a**) and left atrial (**b**) showing recovery from inactivation. Recover was measured using two identical voltage clamp steps to -20 mV from a holding potential of either

-80 , -100 , or -120 mV separated by selected time intervals. The recovery time-course of I_{Na} recorded from the two cell types at the different holding potentials (**c–e**)

Indeed, PV cells had a lower density of both peak and persistent (or late) I_{Na} than atrial cells. Analysis of the biophysical gating parameters showed that PV cells had a more negative steady-state inactivation $V_{1/2}$ and slower recovery from inactivation compared to atrial cells. Examination of the main alpha subunit, Nav1.5, showed lower levels of message (by qPCR) but equivalent levels of the protein (by Western blot) in PV cells. Interestingly, several of the beta subunits were also differentially expressed in the two tissue types although the functional significance of these differences is unknown. The lower I_{Na} density in PV cells may result in a differential response of these tissue types to pathophysiological conditions.

Comparison with previous studies

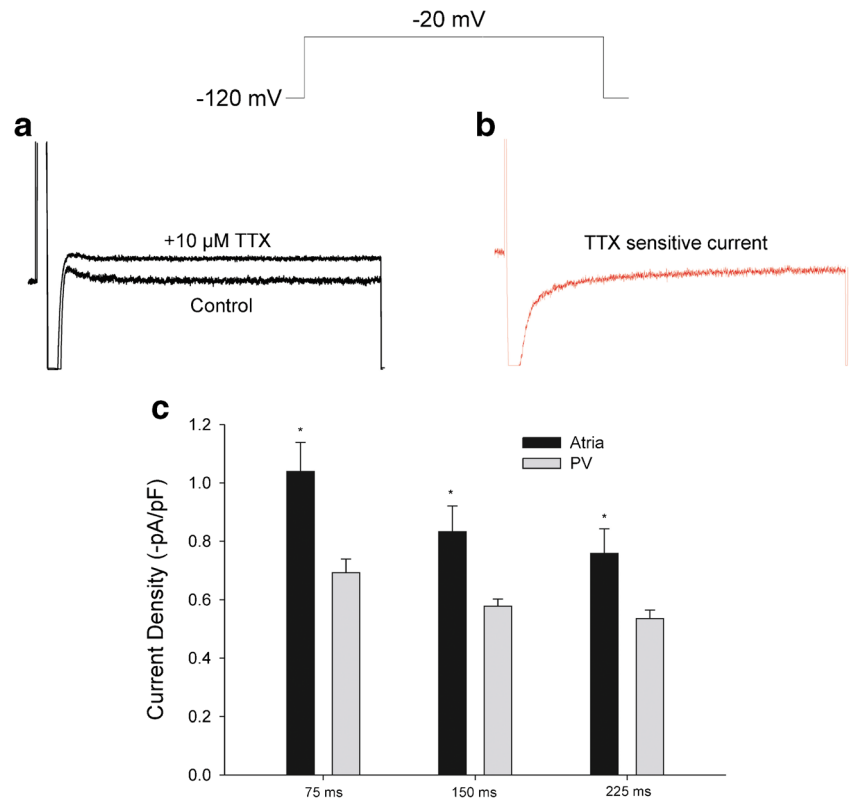
In the canine heart, important regional differences in I_{Na} have been identified and described. For example, we and others have previously shown that I_{Na} in atria had a greater density and more negative steady-state inactivation curve compared to ventricle [5, 7, 27]. Other studies examining tissue-specific differences in I_{Na} have shown that ventricular Epi I_{Na} had a more negative steady-state mid-inactivation potential compared to Endo, but no differences in current density was noted [11]. Previous studies comparing I_{Na} in PV in atria has yielded differing results. For example, there were no observed difference in I_{Na} density between atria and PV cells in canine cardiomyocytes [14]. In contrast, rat myocytes exhibited a

larger peak I_{Na} in PV cells compared with that in atria [22] while the results of our study demonstrate a larger peak and late I_{Na} in atrial cells compared to PV cells. We found that late I_{Na} was smaller in PV compared to atrial cells. Interestingly, both cell types exhibited a larger late I_{Na} compared to ventricular cells under similar recording conditions. Despite the larger late I_{Na} , APD in atrial tissue tends to be much smaller compared to ventricle. The presence of atrial-specific K^+ currents such as the ultrarapid delay rectifier (I_{Kur}) [16] and the acetylcholine sensitive ($I_{K,Ach}$) K^+ current [6, 30] may increase repolarization reserve in atrial tissue and shorten APD compared to ventricle.

Biophysical and molecular analysis of I_{Na}

The α and β subunit composition of I_{Na} differs between PV and atrial cells. It is well established that I_{Na} in cardiac myocytes is not simply the presence of the pore-forming α subunit but that other proteins are involved. Some of these proteins include several β subunits which combine to form the Na^+ channel complex [24]. In addition, I_{Na} in cardiac myocytes is mainly composed of the cardiac isoform (Nav1.5) with a lesser amount of various neuronal isoforms [21, 29]. Interestingly, the mRNA expression of $\beta 1$ – $\beta 4$ subunits was remarkably different with PV cells expressing less $\beta 1$ compared to atrial (Fig. 6). Our qPCR and electrophysiological experiments showed that Na^+ channel current and

Fig. 5 **a** Representative late I_{Na} recorded during a train of five pulses in control solution and after application of TTX ($10 \mu\text{M}$). **b** Subtraction of the traces shown in **a** yielded TTX-sensitive late I_{Na} . **c** Bar graph showing late I_{Na} density in the 2 cell types during the 225 ms pulse to -30 mV . $*P < 0.05$ vs. control



message was lower in PV vs. LA. However, results of our Western blot experiments revealed that both Nav1.5 and Nav β 1 protein was statistically similar. There was a trend that PV contained more Nav1.5 and less Nav β 1 compared to LA. One would expect higher Nav1.5 protein levels to yield a larger I_{Na} , but the lower Nav β 1 may offset this difference. While the β subunits do not generate any current, the presence of β subunits alters the biophysical properties of I_{Na} . Studies have shown that the presence of these subunits can facilitate trafficking of Nav1.5 to the membrane, alter the rate of recovery from inactivation, and shift the steady-state inactivation

curve [23]. In a recent study, Chen et al. [10] investigated the molecular mechanism responsible for the differences in I_{Na} observed in atria vs. ventricular cells. Results of the study showed that Na ν β 2 and Na ν β 4 expression was much lower in atrial tissue. The authors speculate this lower expression of beta subunits is responsible for the distinct biophysical properties of I_{Na} in atria, namely a more negative steady-state inactivation, and a faster activation and inactivation. The authors further demonstrate a differential sensitivity of I_{Na} to the Na $^+$ channel blocker dronedarone [10].

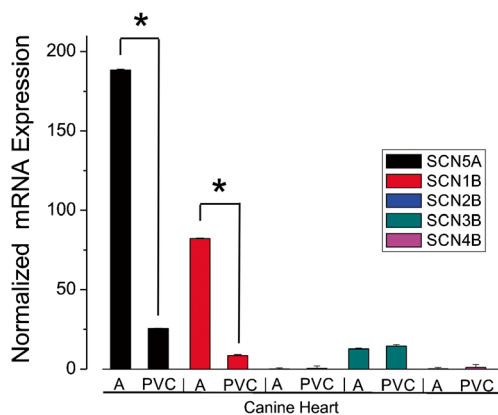
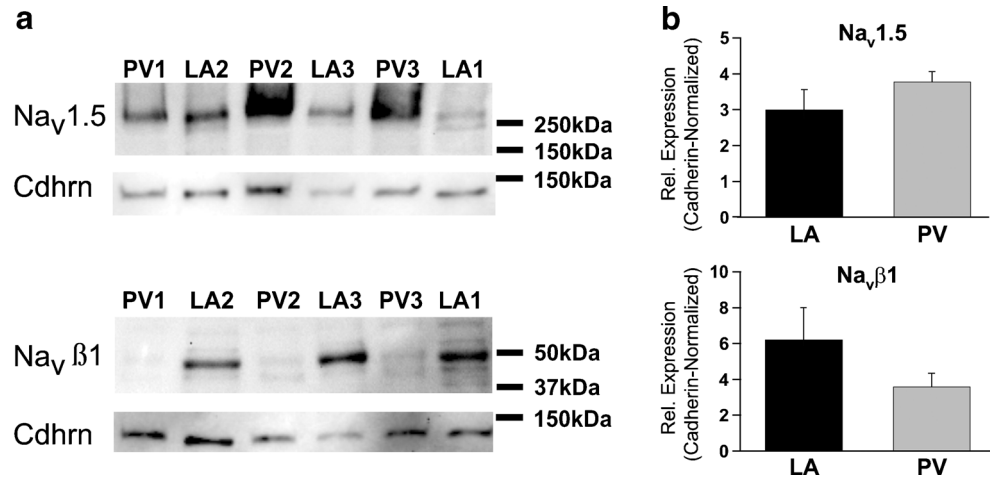


Fig. 6 Bar graph comparing fold changes in the pulmonary vein ($n = 5$) relative to left and right atria ($n = 18$) for five voltage-gated sodium channel genes in the canine heart. Expression was normalized from ΔCt values for each gene against reference gene 18S. $*P < 0.05$

Differences under pathophysiological conditions

Previous studies have found differences in ion channel density between atrial and PV tissue. For example, modeling studies suggested that during atrial fibrillation, there is an attraction of the electrical wavefront to the PV and differences in I_{K1} gradient are critical to the formation of rotors [9]. Although I_{Na} was not evaluated in that study [9], it is established that regional variations in I_{Na} density contributes to dispersion of repolarization and arrhythmia formation [1]. Differences in repolarization gradients may further increase dispersion of repolarization [2]. Our results show there are small but significant differences in the inactivation characteristics, recovery, and density of Na $^+$ channels in the two cell types. Steady-state inactivation in PV cells showed a half-inactivation voltage that is about 2 mV more negative and a recovery from

Fig. 7 **a** Representative Western blots and relative protein level (to Cadherin) of Nav1.5 and Nav β 1 in LA and PV. Each lane represents LA and PV from a different animal. **b** Mean data showing protein levels of Nav1.5 and Nav β 1. Tissue obtained from $n = 3$ animals



inactivation that is slower than that of atrial cells. While these differences may not be important under normal conditions, our results strongly suggest these differences may become important during pathophysiological conditions such as during ischemia or acidosis. This would lead to a greater depression of PV tissue, particularly at depolarized potentials, leading to conduction slowing or block, all of which lead to conditions favorable for the development of re-entrant arrhythmias. Acidosis alone reduces the magnitude of peak I_{Na} by about 40% [31, 33] whereas elevated external K^+ reduces V_{max} of the action potential by leaving a larger pool of Na^+ channels in the inactivated state [11, 17–19].

While our results suggest differences in I_{Na} characteristics between PV and atria can contribute to arrhythmia formation, other mechanisms are also important. Indeed, optical mapping studies of the PV/LA junction have shown regions with longer APDs in close proximity to regions of shorter APDs, creating conditions favorable for the development of reentry within the PV [2]. Interestingly, the same study noted that V_{max} was lower in PV compared to atrial tissue, leading the authors to speculate that I_{Na} may be lower in PV tissue; however, more fibrosis in the PV area may also contribute to slower conduction. Our results demonstrating that I_{Na} is lower in PV tissue supports these observations. In addition, investigations on connexin subtypes revealed PV tissue had lower levels of connexin 40 and similar levels of connexin 43 compared to atrial tissue, suggesting slower conduction through PV tissue [32].

Clinical implications The PV area initiates many AF episodes; successful ablation of the PV area results in suppression and termination of AF episodes in man. Our data demonstrate that differences in early I_{Na} between PV and atrial cells may contribute to a differential response to certain pathophysiological conditions such as ischemia. In this regard, the PV serves

as the classic anatomical barrier surrounded by excitable atrial tissue. We suggest that the lower I_{Na} density in the PV tissue results in a greater functional depression in the PV tissue leading to conditions favorable for the development of re-entrant arrhythmias.

Acknowledgements We are grateful to Judy Hefferon for excellent technical assistance in the isolation of myocytes.

Compliance with ethical standards This investigation conforms to the Guide for Care and Use of Laboratory Animals published by the National Institutes of Health (The Eighth Edition of the *Guide for the Care and Use of Laboratory Animals* (NRC 2011)).

Funding Sources This study was supported by the Free and Accepted Masons of New York, Florida, Massachusetts, Connecticut, Maryland, Wisconsin, Washington, and Rhode Island (to JMC).

Conflicts of Interests The authors declare that they have no conflict of interest.

Reference

1. Antzelevitch C (2005) Role of transmural dispersion of repolarization in the genesis of drug-induced torsades de pointes. *Heart Rhythm* 2:S9–S15
2. Arora R, Verheule S, Scott L, Navarrete A, Katari V, Wilson E, Vaz D, Olgin JE (2003) Arrhythmogenic substrate of the pulmonary veins assessed by high-resolution optical mapping. *Circulation* 107:1816–1821
3. Barajas-Martinez H, Haufe V, Chamberland C, Blais Roy MJ, Fecteau MH, Cordeiro JM, Dumaine R (2009) Larger dispersion of I_{Na} in female dog ventricle as a mechanism for gender-specific incidence of cardiac arrhythmias. *Cardiovasc Res* 81:82–89
4. Biet M, Barajas-Martinez H, Ton AT, Delabre JF, Morin N, Dumaine R (2012) About half of the late sodium current in cardiac myocytes from dog ventricle is due to non-cardiac-type Na^+ channels. *J Mol Cell Cardiol* 53:593–598

5. Burashnikov A, Di Diego JM, Zygmunt AC, Belardinelli L, Antzelevitch C (2007) Atrium-selective sodium channel block as a strategy for suppression of atrial fibrillation: differences in sodium channel inactivation between atria and ventricles and the role of ranolazine. *Circulation* 116:1449–1457
6. Calloe K, Goodrow R, Olesen SP, Antzelevitch C, Cordeiro JM (2013) Tissue specific effects of acetylcholine in the canine heart. *Am J Physiol Heart Circ Physiol* 305:H66–H75
7. Calloe K, Nof E, Jespersen T, Olesen SP, Di Diego JM, Chlus N, Olesen SP, Antzelevitch C, Cordeiro JM (2011) Comparison of the effects of the transient outward potassium channel activator NS5806 on canine atrial and ventricular cardiomyocytes. *J Cardiovasc Electrophysiol* 22:1057–1066
8. Calloe K, Soltysinska E, Jespersen T, Lundby A, Antzelevitch C, Olesen SP, Cordeiro JM (2010) Differential effects of the transient outward K^+ current activator NS5806 in the canine left ventricle. *J Mol Cell Cardiol* 48:191–200
9. Calvo CJ, Deo M, Zlochiver S, Millet J, Berenfeld O (2014) Attraction of rotors to the pulmonary veins in paroxysmal atrial fibrillation: a modeling study. *Biophys J* 106:1811–1821
10. Chen KH, Xu XH, Sun HY, Du XL, Liu H, Yang L, Xiao GS, Wang Y, Jin MW, Li GR (2016) Distinctive property and pharmacology of voltage-gated sodium current in rat atrial vs ventricular myocytes. *Heart Rhythm* 13:762–770
11. Cordeiro JM, Mazza M, Goodrow R, Ulahannan N, Antzelevitch C, Di Diego JM (2008) Functionally distinct sodium channels in ventricular epicardial and endocardial cells contribute to a greater sensitivity of the epicardium to electrical depression. *Am J Physiol Heart Circ Physiol* 295:H154–H162
12. Datino T, Macle L, Qi XY, Maguy A, Comtois P, Chartier D, Guerra PG, Arenal A, Fernandez-Aviles F, Nattel S (2010) Mechanisms by which adenosine restores conduction in dormant canine pulmonary veins. *Circulation* 121:963–972
13. Dumaine R, Cordeiro JM (2007) Comparison of K^+ currents in cardiac Purkinje cells isolated from rabbit and dog. *J Mol Cell Cardiol* 42:378–389
14. Ehrlich JR, Cha TJ, Zhang L, Chartier D, Melnyk P, Hohnloser SH, Nattel S (2003) Cellular electrophysiology of canine pulmonary vein cardiomyocytes: action potential and ionic current properties. *J Physiol* 551:801–813
15. Eldstrom J, Wang Z, Xu H, Pourrier M, Ezrin A, Gibson K, Fedida D (2007) The molecular basis of high-affinity binding of the anti-arrhythmic compound vernakalant (RSD1235) to $K_v1.5$ channels. *Mol Pharmacol* 72:1522–1534
16. Fedida D, Eldstrom J, Hesketh JC, Lamorgese M, Castel L, Steele DF, Van Wagoner DR (2003) $K_v1.5$ is an important component of repolarizing K^+ current in canine atrial myocytes. *Circ Res* 93:744–751
17. Ferrier GR, Moffat MP, Lukas A (1985) Possible mechanisms of ventricular arrhythmias elicited by ischemia followed by reperfusion. Studies on isolated canine ventricular tissues. *Circ Res* 56:184–194
18. Gilmour RF Jr, Evans JJ, Zipes DP (1984) Purkinje-muscle coupling and endocardial response to hyperkalemia, hypoxia, and acidosis. *Am J Phys* 247:H303–H311
19. Gilmour RF Jr, Zipes DP (1980) Different electrophysiological responses of canine endocardium and epicardium to combined hyperkalemia, hypoxia, and acidosis. *Circ Res* 46:814–825
20. Haissaguerre M, Jais P, Shah DC, Garrigue S, Takahashi A, Lavergne T, Hocini M, Peng JT, Roudaut R, Clementy J (2000) Electrophysiological end point for catheter ablation of atrial fibrillation initiated from multiple pulmonary venous foci. *Circulation* 101:1409–1417
21. Haufe V, Cordeiro JM, Zimmer T, Wu YS, Schiccitano S, Benndorf K, Dumaine R (2005) Contribution of neuronal sodium channels to the cardiac fast sodium current I_{Na} is greater in dog heart Purkinje fibers than in ventricles. *Cardiovasc Res* 65:117–127
22. Hutchison L, Rankin A, Drummond R, Rowan E The properties of sodium channels in rat left atrial and pulmonary vein cardiomyocytes. Proceedings of The Physiological Society 31, C07. 1–1-2014. Ref Type: Abstract
23. Isom LL (2001) Sodium channel β subunits: anything but auxiliary. *Neuroscientist* 7:42–54
24. Isom LL, De Jongh KS, Catterall WA (1994) Auxiliary subunits of voltage-gated ion channels. *Neuron* 12:1183–1194
25. Jais P, Hocini M, Macle L, Choi KJ, Deisenhofer I, Weerasooriya R, Shah DC, Garrigue S, Raybaud F, Scavee C, Le Metayer P, Clementy J, Haissaguerre M (2002) Distinctive electrophysiological properties of pulmonary veins in patients with atrial fibrillation. *Circulation* 106:2479–2485
26. Kaab S, Nuss HB, Chiamvimonvat N, O'Rourke B, Pak PH, Kass DA, Marban E, Tomaselli GF (1996) Ionic mechanism of action potential prolongation in ventricular myocytes from dogs with pacing-induced heart failure. *Circ Res* 78:262–273
27. Li GR, Lau CP, Shrier A (2002) Heterogeneity of sodium current in atrial vs epicardial ventricular myocytes of adult Guinea pig hearts. *J Mol Cell Cardiol* 34:1185–1194
28. Livak KJ, Schmittgen TD (2001) Analysis of relative gene expression data using real-time quantitative PCR and the $2^{-\Delta\Delta CT}$ Method. *Methods* 25:402–408
29. Maier SK, Westenbroek RE, Schenkman KA, Feigl EO, Scheuer T, Catterall WA (2002) An unexpected role for brain-type sodium channels in coupling of cell surface depolarization to contraction in the heart. *Proc Natl Acad Sci U S A* 99:4073–4078
30. Mubagwa K, Carmeliet E (1983) Effects of acetylcholine on electrophysiological properties of rabbit cardiac Purkinje fibers. *Circ Res* 53:740–751
31. Murphy L, Renodin DM, Antzelevitch C, Di Diego JM, Cordeiro JM (2011) Extracellular proton depression of peak and late sodium current in the canine left ventricle. *Am J Physiol Heart Circ Physiol* 301:H936–H944
32. Verheule S, Wilson EE, Arora R, Engle SK, Scott LR, Olgin JE (2002) Tissue structure and connexin expression of canine pulmonary veins. *Cardiovasc Res* 55:727–738
33. Yatani A, Brown AM, Akaike N (1984) Effect of extracellular pH on sodium current in isolated, single rat ventricular cells. *J Membr Biol* 78:163–168
34. Zhang Y, Hartmann HA, Satin J (1999) Glycosylation influences voltage-dependent gating of cardiac and skeletal muscle sodium channels. *J Membr Biol* 171:195–207
35. Zygmunt AC, Eddlestone GT, Thomas GP, Nesterenko VV, Antzelevitch C (2001) Larger late sodium conductance in M cells contributes to electrical heterogeneity in canine ventricle. *Am J Phys* 281:H689–H697
36. Zygmunt AC, Nesterenko VV, Rajamani S, Hu D, Barajas-Martinez H, Belardinelli L, Antzelevitch C (2011) Mechanisms of atrial-selective block of sodium channel by ranolazine I. Experimental analysis of the use-dependent block. *Am J Physiol Heart Circ Physiol* 301:H1606–H1614